Time-resolved photoluminescence and X-ray luminescence studies on rare-earth oxysulfide phosphors

Jonathan P. Creasey and Glenn C. Tyrrell*

Applied Scintillation Technologies Ltd.
Harlow, Essex, United Kingdom, CM19 5BZ

ABSTRACT

The use of rare earth oxysulfide-type phosphor screens is commonplace within x-ray scanning instrumentation either in detection or imaging mode. The x-ray phosphors based on praseodymium-doped gadolinium oxysulfide (Gd_2O_2S:Pr) have short decay times to 10% intensity compared to the more well known europium and terbium analogues. The prompt emission of 511nm luminescence from the Pr-ion results in excellent capability for fast scanning x-ray applications in the 20-100μs time frame.

1. INTRODUCTION

X-ray phosphors with high light intensity, relatively fast decay times (<10μs) and a luminescent spectral matching to silicon photodiode arrays are increasingly becoming a necessity for scanning instrumentation for security applications. Popular phosphor hosts for these applications are the rare-earth oxysulfides, e.g. Y_2O_2S and Gd_2O_2S, due to the high x-ray absorption, resulting from their high atomic number (Z) and k absorption edges at 17.0keV and 50.2keV respectively.

Although much information has been published on the photoluminescence of x-ray phosphors and on the properties of these phosphor screens, very little detail on the decay and afterglow behaviour is known. Recent studies of the synchrotron luminescence of Gd_2O_2S:Pr revealed a fast initial decay (<10μs) with significant afterglow [1]. In addition, a survey of Pr-doped phosphors from different manufacturers revealed a profound variation in duration, intensity and dominant visual colour of the afterglow. This variation of performance inevitably influences the reproducible production of high performance screens for sub-100μs response applications.

This paper is focused at assessing the decay and afterglow processes and ascribing the causes of the variation in the afterglow characteristics. A refined decay and afterglow measurement technique is presented that can be applied to phosphors that luminesce over a wide dynamic range of luminescent intensity. Analysis of the effect of doping concentration and its effect on the decay characteristics and luminescence has been measured using (a) integration techniques, and (b) spectral determination of the afterglow characteristics.

The Gd_2O_2S:Pr phosphor system has also been investigated for computed tomography applications by hot isostatic pressing the phosphor to a translucent ceramic [2]. The optimum Pr-doping for luminescent intensity achieved by these authors was 0.1% by atomic fraction. However, the afterglow component was still prominent at this concentration. Reduction of doping concentration resulted in loss of luminescent intensity and extended afterglow.

The major challenge for this dopant is the extent to which light intensity can be maximised whilst minimising the decay constant and suppressing low level afterglow.

* Correspondence: E-mail: g.tyrrell@appscintech.com; Telephone: (0)1279-641234

In *Rare-Earth-Doped Materials and Devices IV*, Shibin Jiang, Editor,
Proceedings of SPIE Vol. 3942 (2000) • 0277-786X/00/$15.00

2. PHOTOLUMINESCENCE

The photoluminescence of Gd_2O_2S:Pr, as excited from 300nm monochromated lamp source, is shown in Figure 1. The dominant emission peak is shown to be at 511nm with further radiative transfer pathways at wavelength ranging up to 780nm. The photoluminescent efficiency of oxysulfide phosphors is known to be linear over a wide range of excitation energy leading to a wide dynamic range of luminescent intensity [3]. This allows confidence to exclude non-linear effects from the experiments.

The UV photoluminescence spectra show identical characteristics to the x-ray photoluminescence spectra. In this study pulsed x-ray excitation was obtained from a Golden x-ray source generating 50 ns square pulses at 150kVp. The efficiency of these phosphors under x-ray excitation is a function of the x-ray absorption, transfer efficiency of the deposited energy to the luminescent centre and then an efficiency function attached to the luminescent centre itself. The light intensity is modified when a luminescent screen is constructed, and this relates to the energy of the x-rays, the thickness of the layer, the particle size of the phosphor and the detailed mechanics of the screen design, i.e. the presence of absorber or reflector layers. These complex issues are not addressed in this paper. Therefore, most data presented in this paper is obtained from UV sources due to the better spectral resolution of this system.

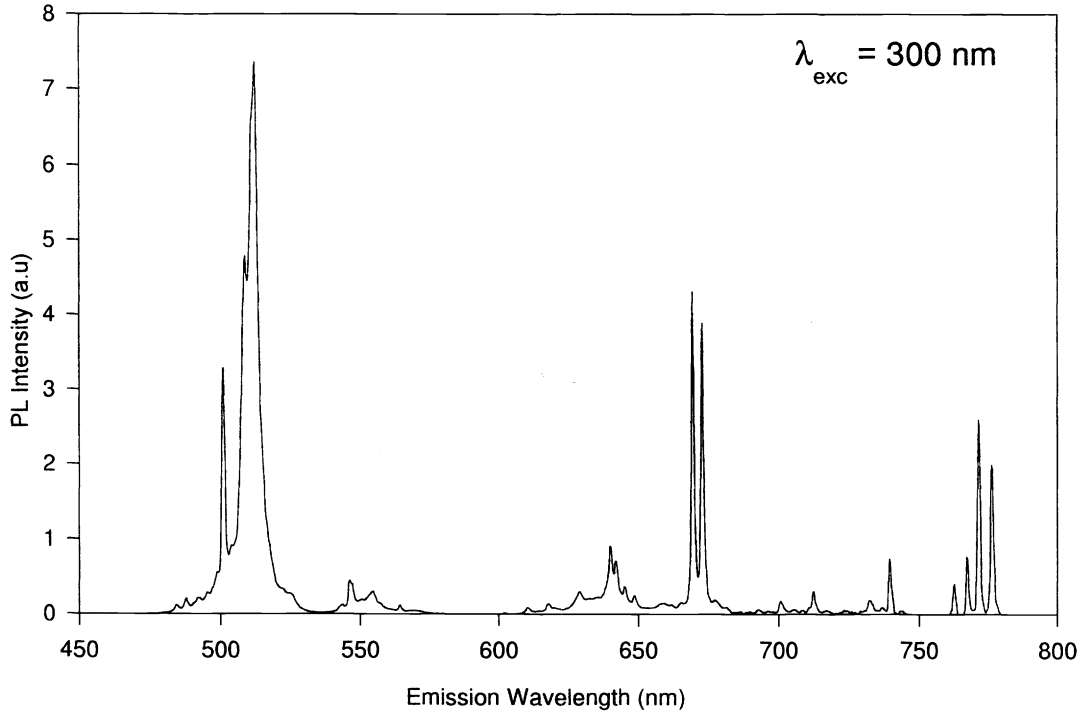

Figure 1: Photoluminescence from a typical Gd_2O_2S:Pr phosphor using monochromated 300nm UV lamp radiation

3. DECAY AND AFTERGLOW MEASUREMENTS

3.1 Prompt decay of luminescence

The decay of a phosphor is an important parameter for imaging or detection devices. Conventional measurements of fast decay in single crystal scintillator typically use the delayed coincidence method of Bollinger and Thomas [4]. This provides good decay information for fast scintillators below 1μs, e.g. cerium-based scintillators [5], but does not cover a sufficient time or gain range to measure within the 1μs to 10ms range that is so often of interest for many commercial instrumentation applications.

The experimental system for the measurement of decay from phosphors is shown in Figure 2. The phosphor sample is mounted within a light tight dark box with a photomultiplier tube, appropriate filters and an optical shutter. The sample is excited using the 337nm emission of a N_2 laser.

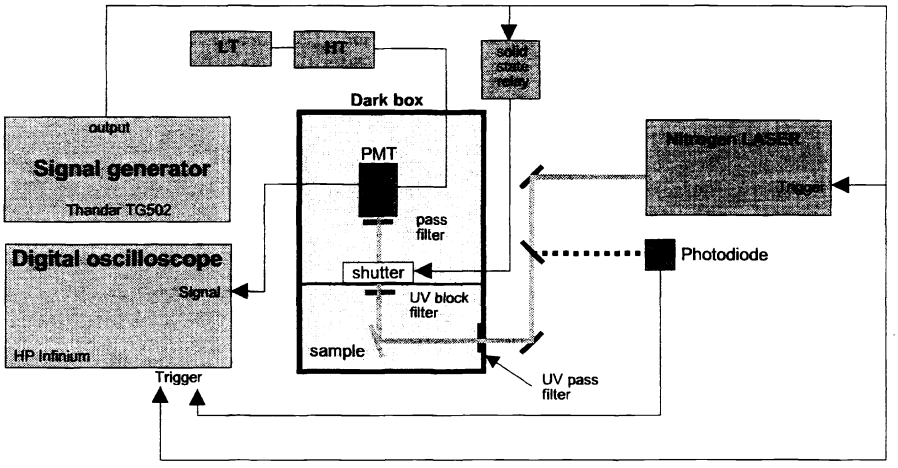

Figure 2: Schematic of photoluminescence system used for both prompt and extended luminescence decay measurements

The prompt decay of Gd_2O_2S:Pr varies as a function of doping concentration. Table 1 shows the effect of shortening the decay constant by increasing the Pr concentration. However, the photoluminescent intensity is significantly attenuated by this process. This clearly impacts on detector design.

Doping concentration (Mol% Pr)	Time constant (1/e) μs	Relative luminescent intensity (%)
0.5	3.75	100
1	3.12	69
2	2.0	45

Table 1: Relationship between Pr-concentration in Gd_2O_2S, decay constant and relative luminescent intensity

3.2 Afterglow of luminescence – Extended Luminescence Decay (ELD)

The purpose of the extended decay curve is to analyse the suitability of a phosphor for a specific dynamic application. The information that can be obtained using this technique includes the measurement of luminescent intensity over an integrated time frame, and an ability to estimate the light leakage into subsequent time frames from the afterglow luminescence.

The set-up for the technique is as previously shown in Figure 2. The sample is excited using a 337nm, 4ns pulsed nitrogen gas laser. The excitation beam passes through a filtered aperture in the dark box that allows only UV in the 337nm region to pass through, thus protecting the photomultiplier from stray ambient light.

The extended decay procedure is built up from a series of measurement stages starting from prompt decay, through intermediate decay processes and finishing with long-lived persistent afterglow.

In the first decay stage the shutter remains open with the laser at a repetition rate of 30Hz. The oscilloscope is triggered from the diode and the photomultiplier terminated with dc-coupled 50Ω. The averaged signal can then be taken at the correct photomultiplier gain to produce decay information from excitation to approximately 20μs. The second stage acquires data from 20μs to 2ms but requires using a different time base.

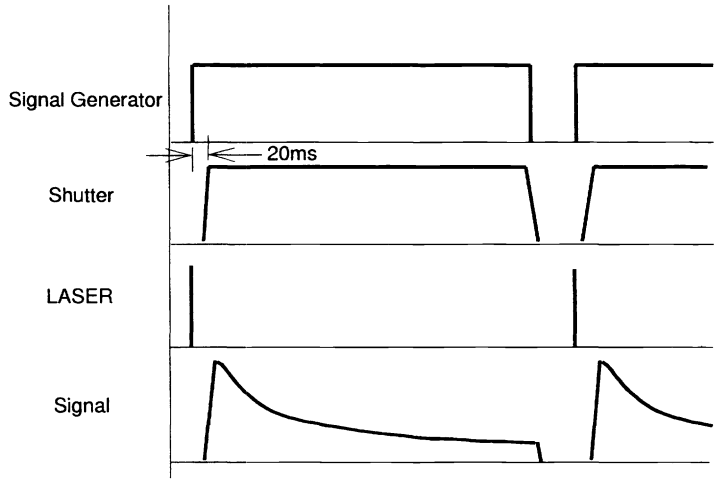

Figure 3: Timing sequence for extended luminescence decay (ELD) procedure

The third stage requires a change in the photomultiplier termination to 1MΩ. Collection of data in the time frame to 2ms to 20ms is valid for this technique. However, fast decay data below 2ms is subject to signal distortion from the reduction in the signal response time.

The fourth and fifth stages of data collection require the use of an optical shutter to remove the high intensity signal from the initial decay component of the praseodymium luminescence. The shutter, oscilloscope and laser are all triggered using the signal generator. The signal timing of the experiment is shown above in Figure 3. This stage captures the afterglow from 50ms (limited by response time of shutter opening) to >100 seconds (signal magnitude dependent). The symmetry of the output from the signal generator is set such that the logic 0 level is short. The activation delay time of the shutter is sufficient to block the first 20-40ms from the decay profile.

The decay curve is extended using a series of parameters that are tabulated (Table 2). This is particularly important because of the precise experimental procedures that are employed in these measurements.

STAGE	Oscilloscope					Photomultiplier tube		Sig. Gen.	LASER	Shutter
	Average	Trigger	Coupling	Timebase	Sensitivity	Filter	HT	Period	Trigger	Status
1	Low	Laser via diode	DC-50Ω	2μs	Set as necessary	Large ND	High	-	Internal 30 Hz	Open
2	High	Laser via diode	DC-50Ω	200μs	1 mV	Large ND	High	-	Internal 30 Hz	Open
3	High	Laser via diode	DC-1MΩ	2ms	1 mV	None	Set as necessary	-	Internal 30 Hz	Open
4	Low	Signal generator	DC-1MΩ	As required	1-10mV	None	High	1s	Signal generator	Signal gen.
5	Med-high	Signal generator	DC-1MΩ	As required	1-5mV	None	High	20s	Signal generator	Signal gen.

Table 2: System parameters for the extended luminescence decay (ELD) procedure

The resultant decay curve for integrated light emitted from a range of Gd_2O_2S phosphors is shown in Figure 4. It can be seen that there is an impressive dynamic range of emission that emanates from these phosphors. This allows sufficient scope to evaluate the integrated light output that falls within a collection frame, and similarly that luminescence that falls within subsequent collection frames. The ability to accurately measure the afterglow characteristics within a specified time frame allows statistical methods to be employed for subtraction of carry-over signal into subsequent frames.

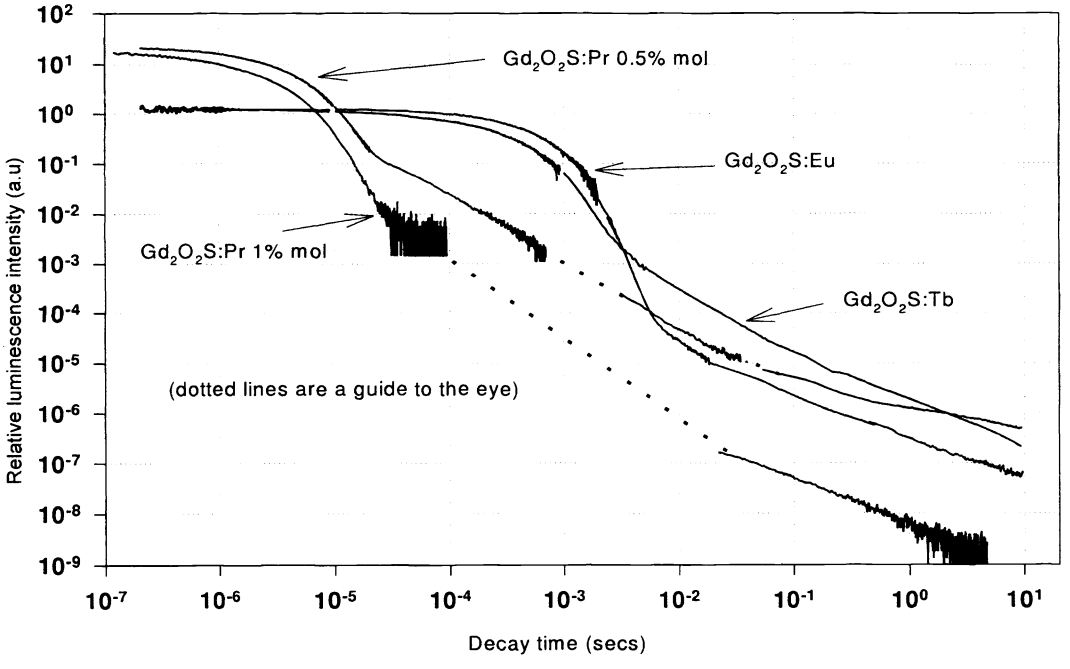

Figure 4: Extended luminescence decay curve from Pr-, Tb-, and Eu-doped Gd_2O_2S phosphors

The effect of increasing doping concentration from 0.5% to 2% reveals a trend of decreasing the decay constant. However, a consequence of this is the reduction in luminescence intensity. This is consistent with typical observations in scintillators, such as increasing Ce^{3+} concentration in Gd_2SiO_5 [6]. The onset of concentration quenching can be described in terms of energy transfer to killer sites (e.g. Eu^{3+}, Gd^{3+}, Tb^{3+}) or by cross relaxation by rare-earth ion pairs (Sm^{3+}, Dy^{3+}). Blasse has suggested a possible cross relaxation mechanism, which varies in influence according to the nature of the crystal lattice [7].

A major consideration in the application of fast decay phosphors is the extent of the afterglow. This has proven problematical for the Pr-doped material. Moy et al reports substantial afterglow, but the dynamic range of the decay is inaccurate due to the limitations of the measurement peak in the 20μs following the excitation.

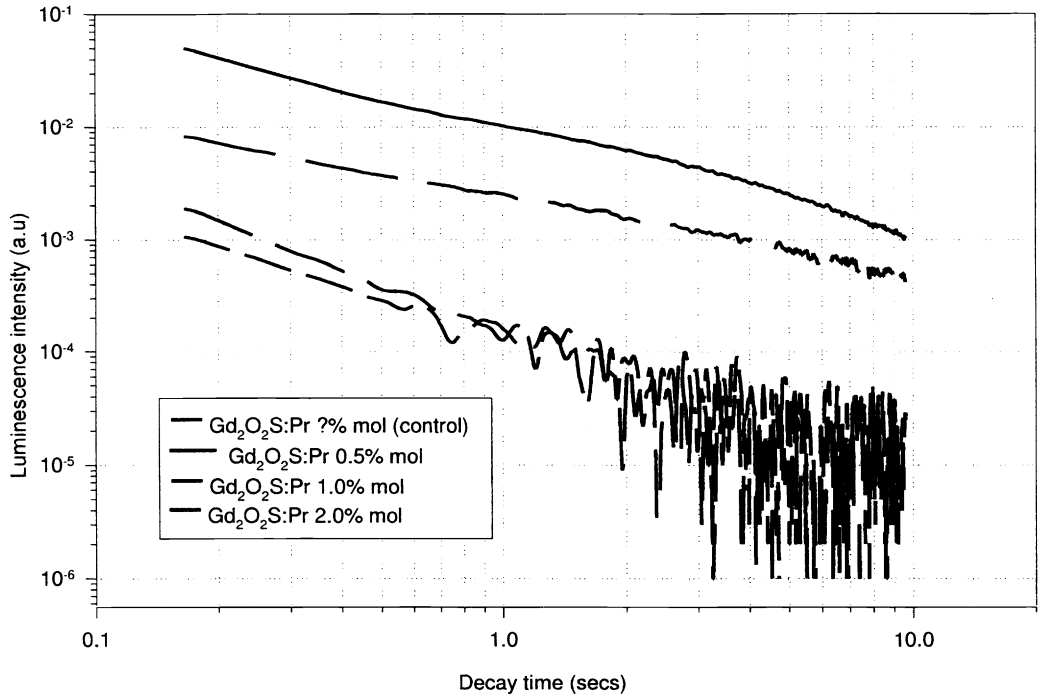

Figure 5: Decay rate of afterglow as a function of differing Pr- concentrations for Gd_2O_2S

By use of a temporally near-gaussian pulsed excitation source (either, nitrogen laser, 4ns, or X-ray, 50ns) it is possible to measure the initial decay component of the Pr ion itself. The time constant varies as a function of doping concentration and as shown previously in Table 1. Figure 5 shows the afterglow decay for several Gd_2O_2S:Pr phosphors with differing Pr concentration. Increasing the Pr concentration depresses the afterglow by several orders of magnitude, which can be extremely significant for fast scanning applications that have measurement cycles of less than 50μs.

The combination of this data shows the difference in prompt decay and afterglow of the Pr ion compared to the more well known Tb and Eu phosphors. Gd_2O_2S:Pr shows a high luminescence output in the <10μs region. However, over longer integration times the Tb and Eu phosphors become the preferred scintillator. The 1 mol% Pr-doped Gd_2O_2S also shows the extent to which afterglow can be suppressed. However, the 0.5 mol5 sample shows pronounced afterglow. This afterglow is spectrally analysed in the following section.

3.3. Spectral resolution of afterglow: Delayed photoluminescence spectroscopy (DPLS)

Conventional measurement of afterglow in fast phosphors is often difficult due to the initial high signal emanating from the excitation pulse through decay to 40 μs. The schematic (Figure 6) shows a set-up for a method that allows the collection of spectral information using a high gain configuration. The sample is excited with a 4ns pulse from a N_2 laser. Fluorescence is collected into a monochromator via an optical chopper, which can also act as a mask from the initial decay from the phosphor. The configuration requires the optical chopper to block the initial decay at the point of triggering. The importance of preventing extraneous light from entering the measurement system cannot be overestimated.

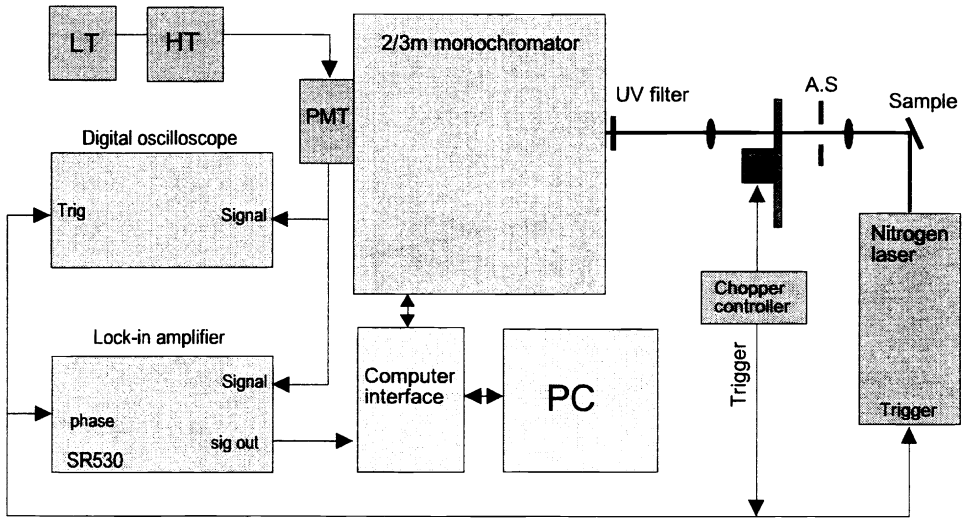

Figure 6: System schematic for the delayed photoluminescent spectroscopy (DPLS) technique

Figure 7 shows DPLS from a 0.25 mol% Pr-doped Gd_2O_2S phosphor. There is a rich diversity of radiative transitions under this high gain condition that do not correspond to the photoluminescence spectra under continuous excitation conditions. The emission peaks assigned in this spectrum can be assigned unambiguously to the presence of europium within the phosphor. Comparison with a Gd_2O_2S:Eu phosphor shows precise spectral matching of the afterglow of the Pr-doped phosphor with the Eu-doped analogue.

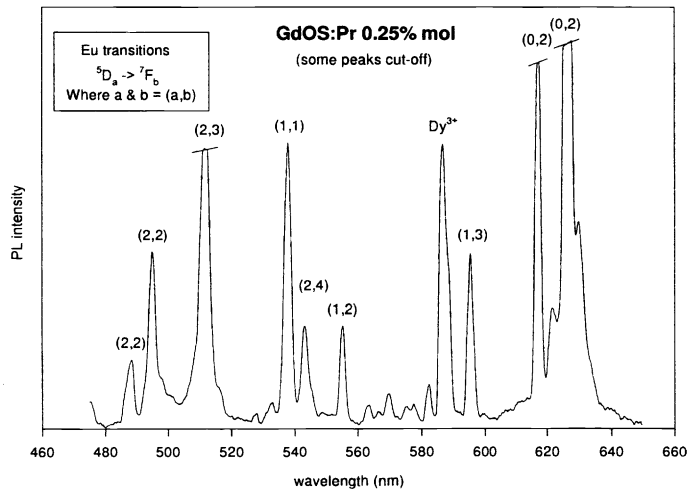

Figure 7: Photoluminescence of afterglow from Gd_2O_2S:Pr phosphor

4. SUMMARY

The use of fast x-ray phosphors is likely to become more commonplace in fast scanning instrumentation, particularly for security applications. This paper outlines the compromises for Gd_2O_2S:Pr in achieving suppression of afterglow, whilst retaining sufficient luminescent intensity for the sensitivity of the silicon detector of choice. In addition, there are underlying processes in phosphor manufacture that are more closely linked to supply of commercial grades of rare-earth precursor oxides that influence the underlying afterglow characteristics of these phosphors.

It is clear that future needs will dictate careful choice of phosphor starting material in addition to the conventional x-ray screen dilemnas, such as compromise of layer thickness, particle size and reflector/absorber options.

ACKNOWLEDGEMENTS

The authors would like to thank G. Sorce of Phosphor Technology Ltd for phosphor samples and J. Vogel of AST for preparation of x-ray screens.

REFERENCES

[1] J.P. Moy, A. Koch and M.B. Nielsen "Conversion efficiency and time response of phosphors for fast X-ray imaging with synchrotron radiation" *Nucl. Instr. Meth.* **A236** (1993) 581

[2] H. Yamada, A. Suzuki, Y. Uchido, M. Yoshida and H. Yamamoto and Y. Tsukuda "A scintillator Gd_2O_2S:Pr, Ce, F for X-ray computed tomography *J. Electrochem Soc.* **136** (1989) 2713

[3] D.E. Husk and S.E. Schnatterly " Photoluminescent efficiency of Y2O2S:Eu and ZnS:Ag phosphors as a function of irradiation intensity over 9 orders of magnitude" *J. Opt. Soc. Am.* **7** (1990) 2226

[4] L.M. Bollinger and G.E. Thomas "Measurement of the time dependence of scintillation intensity by a delayed coincidence method" *Rev. Sci. Instr.* **32** (1961) 1044

[5] W.W. Moses, S.E. Dorenzo, A. Fyodorov, M.Korzhik, A.Gektin, B. Minkov and V. Aslanov "$LuAlO_3$:Ce – A high density, high speed scintillator for gamma detection" *IEEE Trans. Nucl. Sci.* **42** (1995) 275

[6] C.L. Melcher, J.S. Schweitzer, T. Utsu and S. Akiyama "Scintillation Properties of Gadolinium Orthosilicate" *IEEE Trans. Nucl. Sci.* **37** (1990) 161

[7] G. Blasse "Luminescence of inorganic solids from isolated centres to concentrated systems" *Prog. Solid. State. Chem.* **18** (1988) 79